Hollow-Fiber-Based Adsorbers for Gas Separation by Pressure-Swing Adsorption

Xianshe Feng, Chuen Y. Pan, Curtis W. McMinis, John Ivory, and Dave Ghosh
Alberta Research Council, Edmonton, Alta., Canada T6N 1E4

Hollow-fiber-based adsorbers for gas separation by pressure-swing adsorption (PSA) was studied experimentally. The high efficiency of hollow-fiber-based adsorbers for gas separation was illustrated by hydrogen separation using fine-powder-activated carbon and molecular sieve as adsorbents. The adsorption equilibrium and dynamics of the hollow-fiber adsorbers were determined. The pressure drop of the gas flowing through the adsorbers was also examined. The adsorbers were tested for hydrogen separation from nitrogen, carbon dioxide, and a multicomponent gas mixture simulating ammonia synthesis purge gas. The PSA systems using the hollow-fiber adsorbers were very effective for hydrogen purification. The high separation efficiency is derived from the fast mass-transfer rate and low pressure drop, two key features of hollow-fiber-based adsorbers.

Introduction

Pressure-swing adsorption (PSA) is being widely used for gas purification and certain bulk-separation applications. In this process, certain gas components in a mixture adsorb preferentially onto the surface of adsorbent particles, which are often packed in a fixed-bed column. Periodic desorption of the adsorbed species is needed to regenerate the adsorbents and to recover the adsorbate. This can be effected by lowering the pressure of the adsorption column, purging a portion of purified product at a reduced pressure, or a combination thereof. To carry out the separation in a continuous fashion, dual- or multibed systems are often used where each bed undergoes sequential steps of adsorption and desorption. Process modifications, including the incorporation of cocurrent depressurization, pressure equalization, and countercurrent blowdown into the operation cycle, have been developed to improve the separation performance of PSA processes (Yang, 1987; Ruthven, 1984).

The adsorption capability and selectivity of an adsorbent, which are primarily determined by the physicochemical properties of the adsorbent and the fluid mixtures to be separated, are critical to the separation performance. The rate of mass transfer and the pressure drop through the adsorber column, on the other hand, are two important engineering factors that affect the efficiency of PSA processes. The mass-transfer rate is determined by the resistance encountered by the fluid stream during transport between bulk fluid phase and the adsorption surface of the adsorbent. The adsorption rate determines the length of mass-transfer zone in the adsorber and influences the efficiency of adsorbent utilization. Similarly, desorption rate determines the time needed for adsorbent regeneration. A high pressure drop for fluid flow through an adsorber not only leads to pumping or compression costs but also tends to cause attrition of adsorbent particles, uneven distribution of gas flow, and bed lifting (for upflow) or bed crushing (for downflow). Both the mass-transfer rate and the pressure drop are closely related to the size of adsorbent particles (Keller et al., 1987). Almost all industrial adsorbent particles used for practical gas separations are microporous, and the internal surface area is primarily responsible for adsorption. Small particle sizes offer rapid mass transfer and result in a sharp breakthrough curve due to small intraparticle resistance to mass transfer. The smaller the particle sizes are, however, the more closely the particles pack, resulting in an increase in pressure drop. The minimum size of adsorbent particles that can be used effectively in a packed-bed adsorber is limited by the hydrodynamic operating conditions so as to prevent an excessive pressure drop. The commercial adsorbents for fixed-bed operations generally have a particle size larger than 2–3 mm in equivalent diameter.

Pan and McMinis (1992) invented a hollow-fiber device that can be applied to adsorption processes. The invention, as-

Correspondence concerning this article should be addressed to X. Feng.

signed to the Alberta Research Council, uses a bundle of porous hollow-fiber membranes to hold the minute adsorbent particles in place. The fiber wall, with pore openings in the microfiltration range, has minimal resistance to gas flow. The hollow fibers are arranged in a shell-and-tube configuration with proper potting of fiber ends. The adsorbent particles can be confined in either the bore or the shell side, with the gas stream flowing through the other side and yet still maintaining good contact between the gas stream and the adsorbent. The separation occurs primarily by selective adsorption on the adsorbent and not by selective permeation through the fiber wall. Compared to the conventional fixed-bed adsorber, the hollow-fiber device offers numerous advantages. (1) Pressure drop is reduced significantly due to unobstructed passageway for the gas flow. Thus hollow-fiber adsorbers are of special value in some niche applications where low pressure drops are required. (2) Very small adsorbent particles can be used to reduce the intraparticle mass-transfer resistance, and the need for highly porous adsorbent is reduced due to very large specific external areas of extremely fine particles. This broadens the scope of adsorbent materials selection. (3) A more uniform contact of gas with adsorbent is achieved, with the problems associated with gas flow channeling and adsorbent dead-spacing being minimized. (4) Because of low pressure drop and fast mass transfer, fast PSA cycles can be used to enhance process capacity.

It should be pointed out that several issues concerning structure and dimension need to be addressed in selecting the hollow fibers. The fiber wall should be highly porous to reduce the resistance to gas penetration across the wall, and yet the pore size of the fiber wall needs to be sufficiently small to retain the fine adsorbent particles. If mass transfer is severely affected by the resistance of the fiber wall, the performance of the hollow fiber adsorber will be compromised (Gilleskie et al., 1995). Reducing fiber diameter can increase the packing density of the fiber and enhance the overall dispersivity of particle packing in the adsorber. However, the fiber diameter should be significantly larger than the size of the adsorbent particle in order to eliminate the "wall effect." The wall effect is caused by a disparity in the interstitial void fraction of the packed particles. The packing of the particles near the fiber wall is more ordered than in the bulk region of the packed particles, resulting in a higher interstitial void fraction near the wall. The relative size of the particles and the fiber should be controlled to minimize the wall effect, which can produce uneven flow distributions and affect the efficiency of adsorbate-particle contact. Since the fiber wall is supported externally by the adsorbent particles, there is no significant requirement for its physical strength. Consequently, thin-walled hollow fibers are preferred so as to minimize its mass-transfer resistance.

In this study, the high efficiency of hollow-fiber-based adsorbers for gas separation and purification was illustrated. Fine-powdered activated carbon and 5A molecular sieve were chosen as adsorbents. The equilibrium adsorption of CO_2 on activated carbon and N_2 on 5A molecular sieve was measured, and the adsorption dynamics of the hollow fiber adsorbers was determined. The pressure drop of the gas flowing through the adsorbers was also examined experimentally. Finally, the adsorbers were tested for hydrogen purification by the PSA process. It was shown that both fast mass transfer and low pressure drop could be achieved by using hollow-fiber-based adsorbers, resulting in a high separation efficiency of PSA systems.

Experimental Studies

Microporous polypropylene hollow fibers supplied by Hoechst Celanese Corp. (Charlotte, NC) were used in the study. The inside and outside diameters of the fibers are 200 and 260 μm, respectively. The fiber wall had a porosity of 40% with nominal pore dimensions (width $\times$ length) of 0.065 $\times$ 0.19 μm. The hollow fibers were assembled in a bundle and encased in a 1/4-in.-OD (6.4-mm-OD) nylon or copper tubing in a manner similar to a shell-and-tube heat exchanger. The shell side of the module was filled with adsorbent powder by using a proprietary technique to provide dense and uniform packing. The lumina of the hollow fibers provide the passageways for gas flow. The adsorbent particles in the hollow-fiber module are individually free but are collectivity immobilized. Figure 1 shows the hollow-fiber adsorber. Activated carbon (Darco KB) and 5A molecular sieve (Union Carbide) were used as adsorbents for the hydrogen separation tests. The hollow-fiber devices containing activated carbon and molecular sieve are designated as Modules AC and MS, respectively. The sizes of the adsorbent particles and other physical parameters of the adsorbers are summarized in Table 1. The adsorbents were subject to activation at an elevated temperature and with inert gas purging. For convenience of communication, the experimental procedure for characterizing and testing the hollow-fiber adsorbers is described in the following pertinent sections. All the experiments were carried out at ambient temperature (23°C).

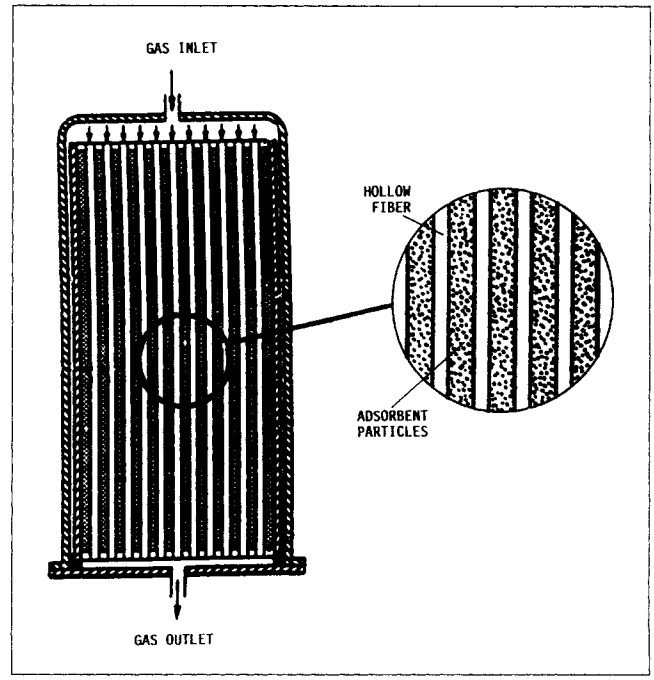

Figure 1. Hollow-fiber adsorber.

The adsorber particles can be loaded either in the shell side or the lumen side.

Table 1. Physical Parameters of Hollow-Fiber Adsorbers

	Module AC	Module MS
ID of module, cm	0.45	0.48
No. of fibers	132	150
ID of fibers, μm	200	200
OD of fibers, μm	260	260
Fiber packing vol. fraction *	0.44	0.44
Active fiber length, cm	64	76
Adsorbent type	Activated carbon	5A molec. sieve
Particle size, μm	< 30	< 10
Packing location	Shell side	Shell side
Particle loading, g	2.3	5.0
Packing density, g/cm^3	0.40	0.64

*Based on fiber OD.

Results and Discussion

Adsorption isotherm

The adsorption isotherms of the adsorbents in the hollow-fiber devices were determined by a gravimetric method using a microbalance. To determine the sorption of N_2 and CO_2 in hydrogen mixtures, the measurements consisted of the following steps.

1. The module weight (W_1) was measured after purging with low-pressure (P_1) hydrogen. Since hydrogen is only slightly adsorptive, the weight of adsorbed hydrogen is considered to be negligible. Thus, $W_1 = W_0 + P_1VM_{H_2}/RT$, where W_0 is the total weight of freshly regenerated adsorbent plus the weight of the fibers, the casing, and the fittings, and ($P_1VM_{H_2}/RT$) represents the weight of hydrogen occupying the void space (volume V) of the module.

2. The module weight (W_2) was measured after purging and pressurizing with high-pressure (P_2) helium, which is nonadsorptive. Then, $W_2 = W_0 + P_2VM_{He}/RT$, where ($P_2VM_{He}/RT$) represents the weight of helium occupying the void space of the module.

3. The module weight (W_3) was measured after purging and repressurizing with the adsorbate-containing gas mixture at pressure P. Then $W_3 = W_0 + W_a + PVM_m/RT$, where W_a is the weight of the adsorbed gas phase, and (PVM_m/RT) represents the weight of the bulk gas phase in the void space of the module. M_m is the average molar mass of the bulk-gas-phase mixture and can be approximated by ΣX_iM_i, where X_i and M_i are the mole fraction and molar mass of component i in the gas mixture, respectively.

4. From the weight difference between W_1 and W_2, the volume of void space in the module V is obtained. Then, from the weight difference between W_3 and W_1, the weight of adsorbed gas W_a can be determined.

In this manner, the amount of adsorbate taken up by the adsorbent at a given pressure and temperature can be obtained. An assumption was made in the preceding procedure that the weight of gas dissolved in the hollow-fiber material is negligible as compared to the adsorbate uptake. Relatively low-pressure hydrogen (700 kPa) and high-pressure helium (1,500 kPa) were used in the measurements because both gases are either slightly adsorptive or nonadsorptive and the molar mass of helium is twice that of hydrogen. This makes the measurements more accurate since the void volume in the adsorber is evaluated from the difference in the weights of gases that occupy the void space. The adsorption isotherms so obtained for CO_2 on activated carbon and N_2 on 5A molecular sieve are shown in Figures 2 and 3, respectively. In both cases, the concentration of bulk gas phase is 10% adsorbate (CO_2 or N_2) and 90% hydrogen. Therefore, from the viewpoint of separating CO_2 and N_2 from H_2, the adsorption isotherms shown in Figures 2 and 3 are a better representation of sorption equilibrium than the isotherms that would be obtained with pure adsorbate gases. It is shown that in the experimental range of measurements, the adsorption of N_2 on the 5A molecular sieve follows the simple Langmuir model (Figure 3). However, the two-parameter Langmuir isotherm fails for the adsorption of CO_2 on the activated carbon, and the hybrid Langmuir-Freundlich model, which is a three-parameter one, was found to correlate the sorption data fairly well (Figure 2). It should be mentioned that the measured adsorption capacity of the molecular sieve crystals is higher than that of pelletized commercial molecular sieve, primarily due to the absence of binding materials in the crystals. The binding materials normally have negligibly small capacities for adsorption of gases.

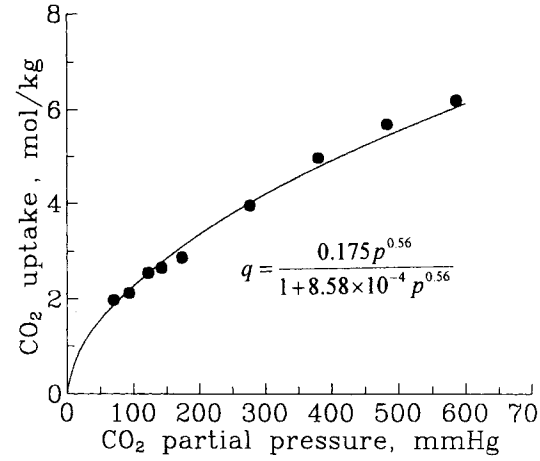

Figure 2. Equilibrium adsorption of CO_2 on activated carbon.

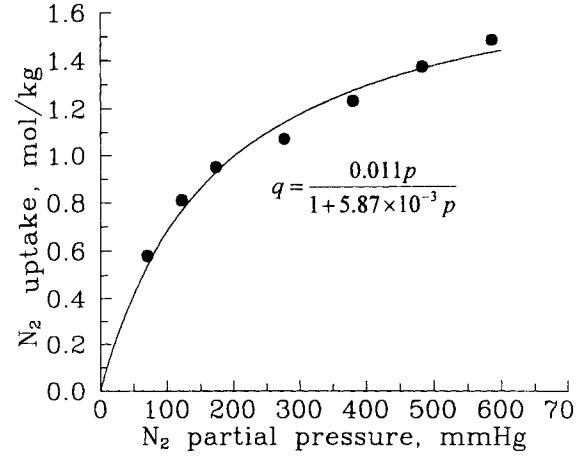

Figure 3. Equilibrium adsorption of N_2 on 5A molecular sieve.

Table 2. Pressure Drop for H_2 Flowing Through Hollow-Fiber Adsorber (Module AC)

Flow Rate, mL(STP)/min	Pres. drop, kPa
200	8.8
400	17.1
600	24.7
800	32.2
1,000	39.2
2,000	71.4
3,000	99.6
4,000	126.8

Pressure drop through adsorber

Low pressure drop through an adsorber is essential for efficient fast-cycle operation of a PSA process. The pressure-drop measurements were performed on the hollow-fiber adsorber module MS using hydrogen at an interstitial gas velocity of up to about 17 m/s. The gas flow rate was controlled by a Matheson mass-flow controller, and the pressure drop was measured by a Rosemount differential-pressure transmitter. The adsorber outlet was open to the atmosphere. Table 2 shows the measured pressure drop at various feed flow rates. For the cases under study where gas flows through the fiber lumen, the pressure drop was found to follow the Hagen-Poiseuille equation for laminar flow:

$$\frac{\Delta P}{L} = \frac{32\mu}{d^2}\left(\frac{\upsilon}{\epsilon_o}\right) = \frac{128RT\mu}{N\pi d^4}\left(\frac{Q}{P_m}\right), \qquad (1)$$

where υ is the average superficial velocity based on the empty cross section of the adsorber, ϵ_o is the fractional volume of the adsorber used for gas flow, that is, the lumen volume per unit adsorber volume, and d is the fiber ID. The quantity υ/ϵ_o represents the interstitial flow velocity. The linear relationship between the pressure drop per unit fiber length, $(\Delta P/L)$, and the molar gas flow rate normalized by its average pressure, (Q/P_m), is illustrated in Figure 4. From Eq. 1 it can be seen that the pressure drop in the hollow-fiber adsorber is proportional to the superficial velocity of gas flow. It depends on gas flow rate and the dimensions and packing density of the hollow fibers, and is not influenced by the particle size and the particle packing density. In the design of a PSA system, the pressure gradient in an adsorbent bed is a critical consideration due to its effects on the power required to operate the system, the life of the adsorbent, and the flow distribution through the bed. The pressure drop through packed-bed adsorbers, which has been a significant problem in both the traditional PSA and the fast-cycle PSA processes (White and Barkley, 1989), can be evaluated by the Ergun equation:

$$\frac{\Delta P}{L} = \frac{150\mu}{d_p^2}\left(\frac{1-\epsilon}{\epsilon}\right)^2\left(\frac{\upsilon}{\epsilon}\right) + \frac{1.75\rho}{d_p}\left(\frac{1-\epsilon}{\epsilon}\right)\left(\frac{\upsilon}{\epsilon}\right)^2, \qquad (2)$$

where d_p and ϵ are the particle diameter and the void fraction in the packed bed, respectively. This equation predicts that the pressure drop is a quadratic function of the interstitial velocity of gas flow (υ/ϵ) and is dependent on the particle size (d_p) and the particle packing density (ϵ). In order to maintain a low pressure drop in a packed bed, either a slow feeding velocity or a large particle size should be used. It has been estimated that when the fiber inner diameter and the particle size are equal for a gas flowing at the same superficial velocity through a fiber adsorber and a packed-bed adsorber whose fractional void volume for gas flow is $\epsilon = \epsilon_o = 0.4$, the pressure drop of the fiber adsorber is about one-tenth that produced by the packed bed (Gilleskie et al., 1995). It can further be estimated that at normal gas feeding rates, when fine particles (such as those used in the current study) are used, the pressure drop in a packed-bed adsorber can be several orders of magnitude larger than in a hollow-fiber adsorber. That the hollow-fiber adsorbers have low pressure drops is one of the key advantages over the fixed-bed adsorbers. Not only are the compression costs and particle attrition reduced, very fine particles can be used at an operating pressure that is otherwise unacceptably high.

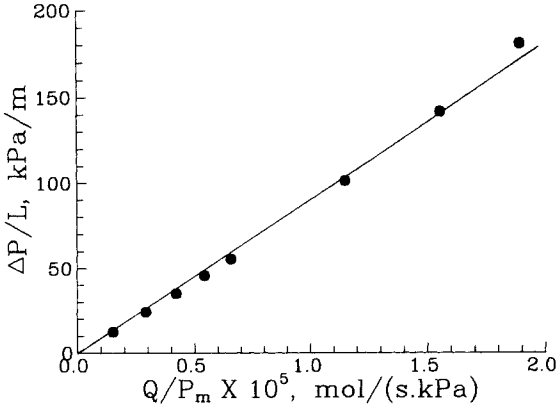

Figure 4. Pressure drop vs. molar-gas flow rate normalized by average pressure.

Gas flowed through fiber lumina, and particles were packed in the shell side.

Mass-transfer characteristics

Adsorption and desorption tests were performed at constant pressures to investigate the mass-transfer characteristics of the hollow-fiber adsorbers. The adsorber was prepressurized with pure hydrogen at the same pressure at which the experiment was to be run. Then the gas mixture was fed to the adsorber, and adsorption was initiated. After the entire adsorber had been fully saturated with adsorbate, pure hydrogen was switched to the adsorber and desorption was thus started under hydrogen purging. A two-position valve was used to switch the gas streams at the adsorber inlet, and a Gow-Mac thermal conductivity gas analyzer monitored by a data-logging computer was used to measure the composition of gas effluent from the adsorber outlet continuously. The test system was plumbed with 1.08-mm-ID stainless-steel tubing to reduce the time lag of measurements. The pressure of the gas sample exiting the adsorber had to be reduced before entering the gas analyzer for composition analysis. This was done by using a short length of 0.13-mm-ID stainless-steel capillary tubing, instead of using a throttling valve that generally has a significant holdup volume.

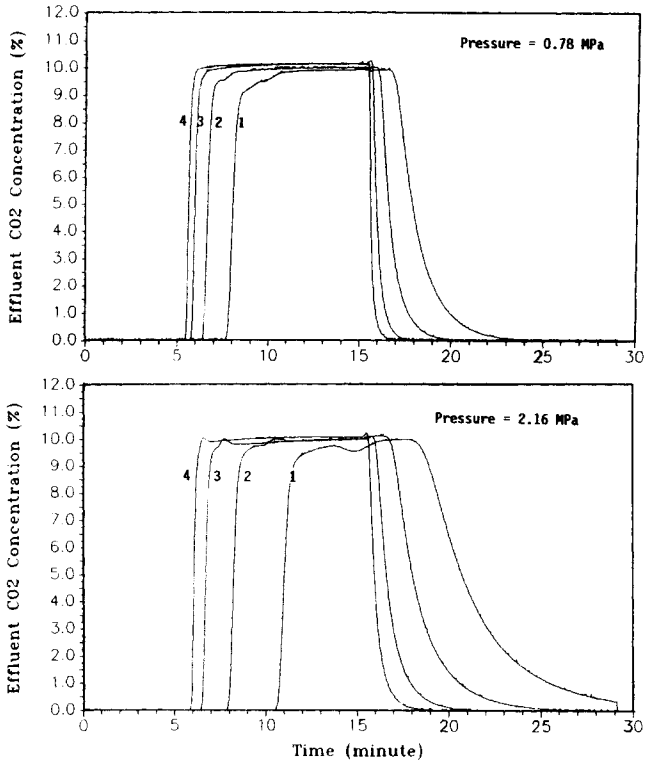

Figure 5. Adsorption/desorption dynamics of CO_2 on activated carbon in hollow-fiber adsorber (Module AC).

Feed gas, 10% CO_2 in hydrogen; flow rate, (1) 250, (2) 500, (3) 1,000, and (4) 2,000 mL(STP)/min. [1 mL(STP)/min = 7.44×10^{-7} mol/s].

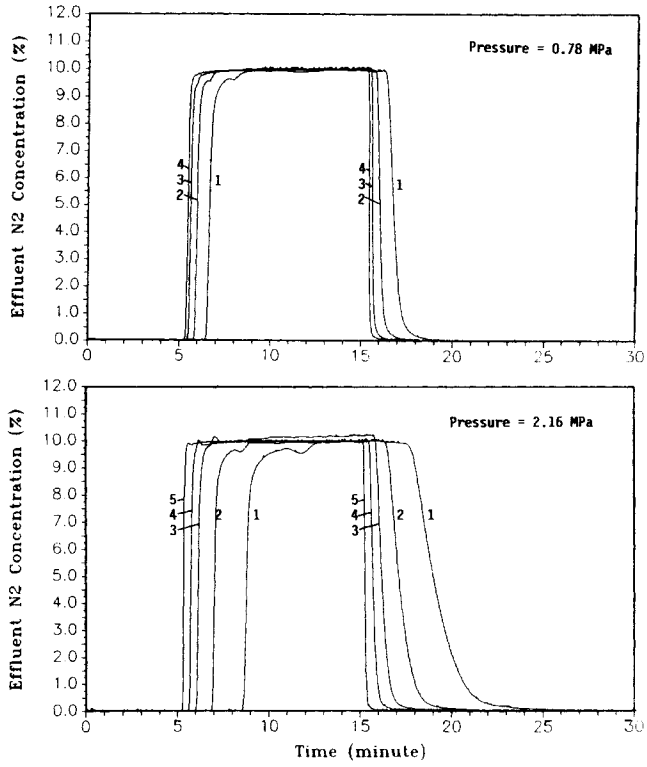

Figure 6. Adsorption/desorption dynamics of N_2 on 5A molecular sieve in hollow-fiber adsorber (Module MS).

Feed gas, 10% N_2 in hydrogen; flow rate, (1) 250, (2) 500, (3) 1,000, (4) 2,000 and (5) 4,000 mL(STP)/min. [1 mL(STP)/min = 7.44×10^{-7} mol/s].

Figures 5 and 6 show the measured sorption/desorption characteristics of CO_2 on activated carbon and N_2 on 5A molecular sieve in the hollow-fiber adsorbers at different gas pressures and flow rates. The time axis in the figure has accounted for the time lags due to system plumbing and detector response, and thus shows the adsorption/desorption time on a relative scale. When the gas mixture CO_2/H_2 or N_2/H_2 is fed to an adsorber, CO_2 or N_2 is preferentially adsorbed. As the gas influent flow continues, the concentration front of the adsorbate in the adsorber advances toward the outlet end of the adsorber, and eventually breakthrough of the adsorbate occurs. Then the adsorber is gradually saturated with adsorbate, and the gas effluent exiting the adsorber becomes less depleted in the more strongly adsorbed species. The shapes of the adsorption/desorption breakthrough curves reflect the mass-transport process in the adsorber and the nature of adsorption equilibrium. From Figures 5 and 6 the following general observations can be made.

1. The adsorption breakthrough curves are virtually of shock-type waves, a feature that is typical of equilibrium adsorption for favorable isotherms with negligible mass-transfer resistance.

2. The adsorption breakthrough time decreases with an increase in the molar flow rate of gas influent. This agrees with physical reasoning that a high gas feeding rate leads to fast saturation of adsorbent with the adsorbate. On the other hand, at a given molar flow rate of gas influent, an increase in operating pressure increases the adsorption capacity of the adsorber, resulting in an increase in the adsorption breakthrough time. For desorption, the opposite is true.

3. The adsorption breakthrough curves show an approximate constant pattern, whereas the desorption breakthrough curves show a proportionate pattern behavior. In contrast to the sharp breakthrough curve for adsorption, the breakthrough curve for desorption is elongated.

The last observation is due to the fact that for the favorable isotherms (see Figures 2 and 3), the movements of concentration fronts for adsorption and desorption in the adsorber are dramatically different. Based on the equilibrium theory, the propagation velocity of a concentration front is inversely proportional to the slope of the sorption isotherm at that point (Basmadjian, 1997). Consider a favorable adsorption isotherm. During adsorption, the propagation velocity of a concentration front progressively increases, because high concentration fronts move faster than low concentration fronts. Consequently, the concentration profile is self-sharpening, and eventually it approaches the limit of discontinuity as a shock wave. On the other hand, the movement of the concentration front during desorption is gradually slowed down. The desorption of the initial parts of the loaded sorbates, which corresponds to fast propagation velocity due to the low-slope segments of the isotherm, is relatively quicker than the desorption of the subsequent portions, leading to a continually broadening concentration front. It should be mentioned that the kinetic effect (mass-transfer resistance), if present, may retard adsorption/desorption, but the funda-

mental difference between the features of adsorption and desorption concentration fronts still holds.

The adsorption/desorption breakthrough curves represent the adsorber dynamics for the given system at the given operating conditions. They are important to the process design since the adsorption breakthrough time determines the adsorption time in a PSA cycle and the desorption breakthrough time determines the desorption time and the purge-gas consumption.

The equilibrium adsorption data in Figures 2 and 3 can be used to calculate the adsorption/desorption breakthrough curves. Prediction of performance of the hollow-fiber adsorbers, which is not attempted in this study, could be made on the basis of equilibrium theory because of the negligible resistance to mass transfer.

Pressure swing adsorption

An instrumented bench-scale pressure swing adsorption system was set up to test the hollow-fiber adsorbers for hydrogen purification. The system consisted of several timer-controlled multiport switching valves, an on-line thermal conductivity analyzer (Gow-Mac) monitoring hydrogen concentration continuously, and a data-logging computer. To illustrate the potential of the hollow-fiber devices for PSA separation, a few gas mixtures and PSA configurations were selected, and the results are presented below. All the experimental data on the PSA performance were obtained at cyclic steady-state conditions, that is, both product throughput and concentration were invariant with the operation cycles. In general, a steady-state operation of the cyclic system was established within 30 min.

H_2/CO_2 Separation by PSA Using Hollow-Fiber Adsorber (Module AC). The PSA system was designed to use a single adsorber and two storage vessels to simulate the typical four-bed system (Wagner, 1969) that covers the basic steps of high-pressure adsorption, cocurrent depressurization, countercurrent blowdown and purge, and repressurization by pressure equalization. The storage vessels were used to store a portion of the pressurized gas from the adsorber, and the gas was then used to purge and repressurize the adsorber. The volumes of the two storage vessels were the same and equal to that of the void space in the adsorber. The operating sequence of PSA, shown in Figure 7, includes the following steps: (1) adsorption of high-pressure feed gas for a predetermined period of time to produce purified gas, which is withdrawn from the outlet end of the adsorber; (2) depressurization of the gas retained in the adsorber into a storage vessel (V1); (3) switching this storage vessel (V1) with the other (V2) for further depressurization of the adsorber; (4) venting the gas remaining in the adsorber from the inlet end of the adsorber; (5) purging the adsorber with the gas stored in storage vessel V2; (6) pressurizing the adsorber with the gas stored in vessel V1; and (7) further pressurizing the adsorber to feed pressure with a portion of purified high-pressure product gas, and the gas remaining in the storage vessel is removed as low-pressure product. The adsorber is now ready for the next cycle. Note that using the effluent gas from one bed to purge and repressurize other beds improves the product recovery and conserves the mechanical energy contained in the compressed gas (Yang, 1987). The final repressurization of the

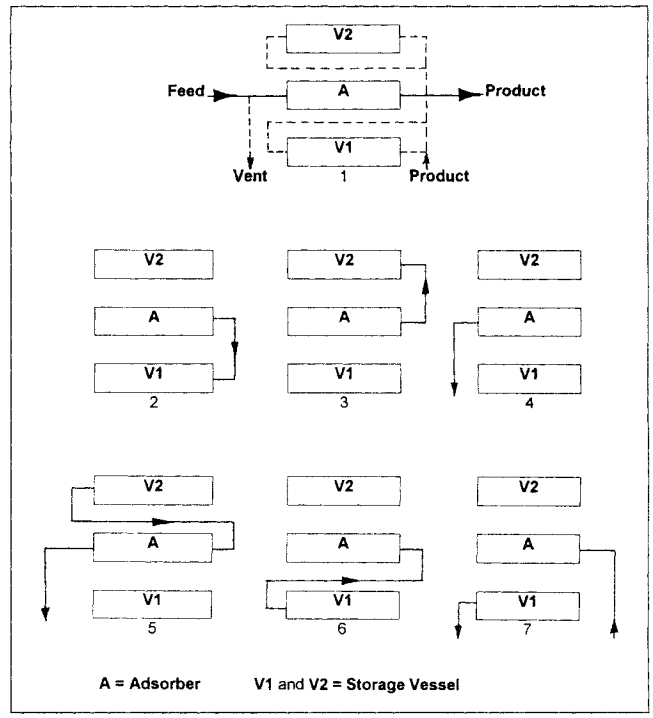

Figure 7. Operating sequence of a single-adsorber pressure-swing adsorption process.

adsorber was completed with the purified high-pressure product to assure product purity. During the experiments, the feed-gas concentration and pressure were maintained constant (10% CO_2, 2.16 MPa), and the feed flow rate was varied. The maximum feed flow rate at a predetermined period of adsorption time without causing CO_2 breakthrough from the adsorber outlet was measured.

The experimental data are shown in Table 3, which reveals that the highest feed flow rate without CO_2 breakthrough is inversely proportional to the adsorption step time, and that under the given operating conditions the hydrogen recovery is virtually the same for all of these flow rates. These results indicate that by using hollow-fiber adsorbers, the PSA cycle time can be reduced significantly to increase the feed gas throughput without losing separation efficiency. Thus, for a given separation task, the adsorber size can be minimized by operating the PSA system at high cycling frequencies. The high adsorption efficiency at fast adsorption cycles and high feed throughput is made possible by the use of a hollow-fiber-based adsorption unit containing minute adsorbent particles due to fast mass transfer and low pressure drop.

Table 3. Test Results of H_2/CO_2 Separation Using Hollow-Fiber Adsorber (Module AC)*

Adsorption Step Time, s	Max. Feed Rate without CO_2 Breakthrough, 10^{-4} mol/s	Hydrogen Recovery, %
10	26.8	76
17	14.9	76
36	7.44	76
72	3.72	76
120	2.23	76
180	1.49	76

*Feed concentration CO_2 10%, pressure 2.16 MPa.

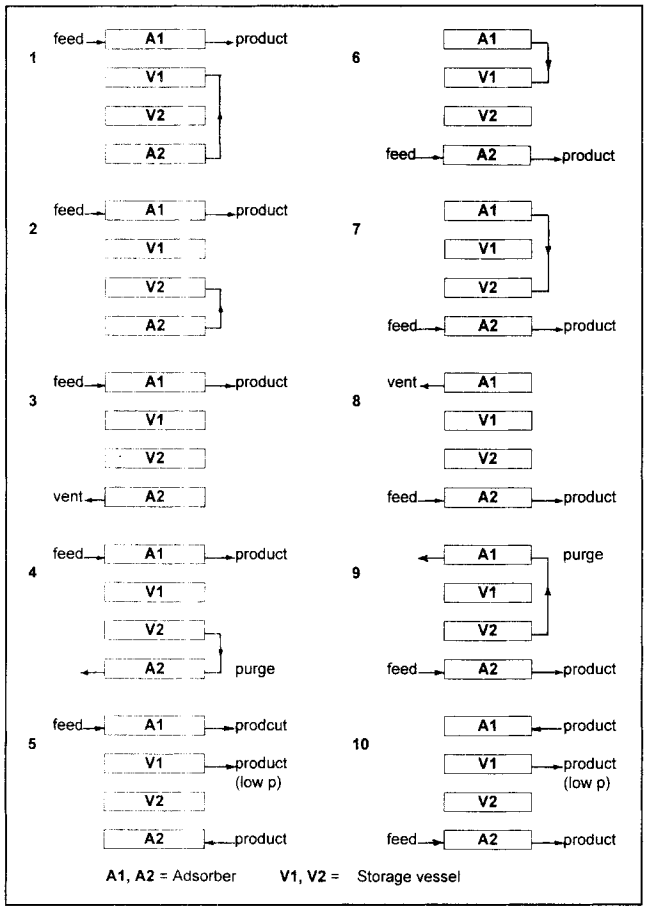

Figure 8. Operating sequence of a dual-adsorber pressure-swing adsorption process.

Table 4. Description of Sequential Steps for the Dual-Adsorber PSA System

Adsorber A1	Adsorber A2
Gas feeding through the inlet of adsorber, high-pressure adsorption, and removal of purified product from the outlet end of adsorber	Depressurization by admitting the gas from adsorber outlet into storage vessel V1 Further depressurization of gas into storage vessel V2 Vent the gas remaining in the adsorber from the inlet end Purge with gas stored in vessel V2 in a direction countercurrent to gas flow in adsorption step Pressurization with a portion of high-pressure product; removal of the gas remaining in storage vessel V1 as low-pressure product
Depressurization by admitting the gas from adsorber outlet into storage vessel V1 Further depressurization of gas into storage vessel V2 Vent the gas remaining in the adsorber from the inlet end Purge with gas stored in vessel V2 in a direction countercurrent to gas flow in adsorption step Pressurization with a portion of high-pressure product; removal of the gas remaining in storage vessel V1 as low-pressure product	Gas feeding through the inlet of the adsorber, high-pressure adsorption, and removal of purified product from the outlet end of adsorber

H_2/N_2 Separation by PSA Using Hollow-Fiber Adsorber (Module MS). The bench-scale PSA system was modified to accommodate two adsorbers. The modified system allows the cyclic PSA process to be carried out in a continuous fashion so as to provide a more accurate simulation of the industrial multibed system. The operating sequence of the dual-adsorber PSA system is shown in Figure 8; a detailed description of the cycle steps is presented in Table 4. The PSA system was tested at a cycle time of 22 s with feed pressures ranging from 0.78 to 2.16 kPa and compositions in the range of 5–20% N_2. During the high-pressure adsorption step, the adsorber was at feed pressure. The gas pressure in the adsorber was reduced by 50% when it was depressurized into the storage vessels whose volumes were the same as and equal to the void volume in the adsorber. The typical test results are summarized in Table 5. It should be mentioned that the product concentration during the cyclic operation of PSA also experiences a cyclic variation, as shown in Figure 9. Installing a surge tank in the product sample line will smooth the concentration variation. In the present study, a 40-mL sample

Table 5. Test Results of Dual-Adsorber PSA System for H_2/N_2 Separation Using Module MS*

Feed Pres. (MPa)	Feed Conc. (N_2%)	Feed Flow Rate (10^{-4} mol/s)	Product Conc. (H_2%)	Hydrogen Recovery (%)	Feed Throughput (mol/s·kg Adsorbent)
2.16	10	8.93	100**	72.3	0.178
2.16	10	9.67	99.88	75.2	0.193
1.48	10	5.95	100**	70.6	0.119
1.48	10	8.18	99.40	81.7	0.164
1.48	20	5.21	100**	64.8	0.104
1.48	20	5.95	99.80	70.6	0.119
1.48	5	6.70	100**	75.1	0.134
1.48	5	8.93	99.40	84.1	0.179
0.78	10	2.83	100**	67.6	0.057
0.78	10	4.46	99.80	83.7	0.089

*Wagner cycle simulated by using two adsorbers and two storage vessels at a cycle time of 22 s.
**No nitrogen was detected in the product streams.

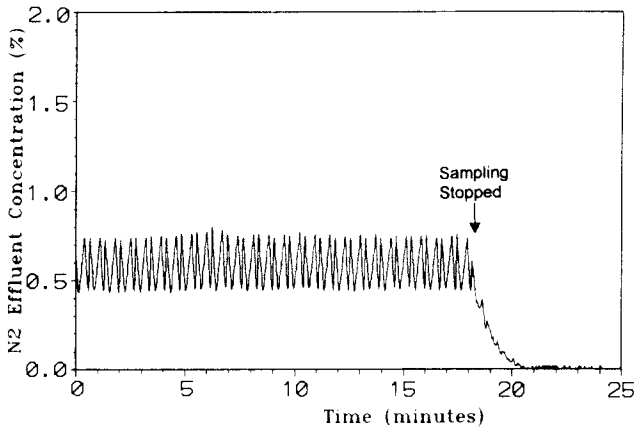

Figure 9. Cyclic change of product concentration during PSA operation.

bottle was used as the surge tank to obtain the volume-averaged concentration.

It can be seen from Table 5 that the product purity generally (1) decreases with an increase in feed flow rate or feed concentration, and (2) increases with a decrease in operating pressure for adsorption. There exists a trade-off between product purity and recovery; either a high recovery or a high purity can be obtained, but seldom both. These results are consistent with the general observations in conventional PSA systems. The data shown in Table 5 indicate that the hydrogen recovery of the hollow-fiber-based PSA system is comparable to the conventional fixed-bed PSA system, but with a much smaller adsorber size.

H_2 Separation from Simulated Purge Gas of Ammonia Synthesis (Module MS). The dual-adsorber PSA system discussed earlier was further tested for hydrogen separation from a multicomponent gas mixture, which was a simulated purge gas of an ammonia reactor loop. The gas composition was as follows: hydrogen, 60%, nitrogen, 20%, methane, 10%, argon, 10%. The test pressure was limited to 2.16 MPa in this study due to the operating pressure limitation of the multiport switching valves used in the PSA system. Other operating conditions were the same as those used in the hydrogen/nitrogen separation tests just described, except that the hydrogen concentration in the product was measured by a Varian gas chromatograph equipped with a thermal-conductivity detector. Table 6 shows the test results. It is shown that at a feed throughput of 0.15 mol/(s·kg-adsorbent), a hydrogen purity of over 97% with a recovery of 42% can be achieved. Increasing the feed throughput to 0.22 mol/(s·kg-adsorbent) increases product recovery to 71%, but at the expense of lowering the product purity (89%). Both the hydrogen purity and recovery are lower as compared to those for separating H_2 from N_2. This is primarily due to the low capacity of the adsorbent to adsorb argon. It should be noted that the limitation of 2.16-MPa feed pressure severely limited the separation performance of the PSA system. The pressure of purge gas in ammonia synthesis is usually available at about 14 MPa. In actual applications, the separation performance of the hollow fiber-based PSA is expected to be improved significantly by using a higher feed pressure.

Table 6. Test Results of H_2 Separation from Simulated Ammonia Synthesis Purge Gas*

Feed Flow Rate (10^{-4} mol/s)	Product H_2 Purity (%)	H_2 Recovery (%)	Feed Throughput (mol/s·kg Adsorbent)
7.44	97.1	42	0.149
11.2	89.0	71	0.223

* Feed composition: 60% H_2, 20% N_2, 10% CH_4, and 10% Ar; pressure, 2.16 kPa.

Conclusions

Hollow-fiber-based adsorbers containing minute adsorbent particles on the shell side were studied experimentally. Hydrogen separation by PSA using activated carbon and 5A molecular sieve was chosen to test the performance of the hollow-fiber adsorbers. The adsorption isotherms of CO_2 on activated carbon and N_2 on 5A molecular sieve were measured, and the adsorber dynamics characterized by the adsorption/desorption breakthrough curves were determined. It was shown that the hollow-fiber adsorbers had a large gas-processing capacity per unit weight of adsorbent.

Due to the fast mass-transfer rate and the low pressure drop, which are two key features of the hollow-fiber adsorbers, the feed-gas throughput is essentially proportional to the frequency of the adsorption cycle. Thus for a given separation task, the adsorber size can be minimized by operating the PSA system at high cycle frequencies. Experiments with hydrogen separation from nitrogen, carbon dioxide, and a multicomponent gas mixture, which simulated ammonia synthesis purge gas, showed that PSA systems using the hollow-fiber adsorbers are very effective for hydrogen separation and purification.

Notation

N = number of fibers in hollow-fiber adsorber
ΔP = pressure drop through adsorber, Pa
R = ideal gas constant
T = temperature, K
μ = viscosity, Pa·s
ρ = density, kg/m^3

Literature Cited

Basmadjian, D., *The Little Adsorption Book: A Practical Guide for Engineers and Scientists*, CRC Press, Boca Raton, FL (1997).
Gilleskie, G. L., J. L. Parker, and E. L. Cussler, "Gas Separation in Hollow-Fiber Adsorbers," *AIChE J.*, **41**, 1413 (1995).
Keller, G. E., R. A. Anderson, and C. M. Yon, "Adsorption," *Handbook of Separation Process Technology*, R. D. Rousseau, ed., Wiley-Interscience, New York, p. 644 (1987).
Pan, C. Y., and C. W. McMinis, "Hollow Fiber Bundle Element," U.S. Patent No. 5,139,668 (1992).
Ruthven, D. M., *Principles of Adsorption and Adsorption Processes*, Wiley-Interscience, New York (1984).
Wagner, J. L., "Selective Adsorption Process," U.S. Patent No. 3,430,418 (1969).
White, D. H., Jr., and P. G. Barkley, "The Design of Pressure Swing Adsorption Systems," *Chem. Eng. Prog.*, **85**(1), 25 (1989).
Yang, R. T., *Gas Separation by Adsorption Process*, Butterworth, Stoneham, MA (1987).

Manuscript received Feb. 11, 1998, and revision received Apr. 6, 1998.